

Parameter Optimization of Hall Effect Gear Tooth Speed Sensors

Junwen Lu ^(1/2) and Ji-Gou Liu⁽¹⁾

(1) ChenYang Technologies GmbH & Co. KG., Markt Schwabener Str. 8, 85464 Finsing, Germany, Email: louis.lu@chenyang.de , jigou.liu@chenyang-ism.com

(2) University of Shanghai for Science and Technology, 200093 Shanghai, China

Abstract

In this paper relevant parameters, such as sensing distance, duty cycle and phase drift of Hall Effect gear tooth speed sensors are optimized by magnetic field analysis, experiments and by using proposed mathematical models. The optimization results are applied to the performance improvement of Hall Effect gear tooth sensors CYGTS101DC and CYGTS104U. Experiment results show that the optimized sensors CYGTS101DC-S and CYGTS104X have better performances than those of sensors 1GT101DC and SNDH-T4I-G01.

1. Introduction

Magnetic speed sensors are widely used for rotational speed measurements in industrial automation, motor drives, intelligent motion, electric bikes and automotive industry, especially electric automobile, for testing, controlling and monitoring engines, motors, generators, and spindles of different rotating machines.

The most used magnetic speed sensors are magnetic encoders, magnetoresistive gear tooth sensors and Hall Effect gear tooth sensors etc. In a magnetic encoder measuring system a multipolar permanent ring magnet or assembly is mounted on a rotary spindle. The magnetic pole change during the spindle rotation is detected with a Hall Effect switch IC or magnetoresistive switch IC. The encoder generates output impulses according to the pole change period of the multipolar magnet. The magnetic encoder has lower resistance to magnetic disturbances because the most material of the multipolar magnet is weak isotropic hard ferrite. Therefore a magnetic encoder is usually assembled in a soft magnetic case in order to shield the magnetic disturbances from environments. This causes encoders relative high manufacturing costs.

A gear tooth rotational speed measuring system consists of a gear tooth sensor and a target wheel. One or two detectors and a permanent magnet (NdFeB or SmCo) are built in the gear tooth sensor. A magnetoresistive gear tooth sensor uses magnetoresistive sensors as detectors while a Hall Effect gear tooth sensor takes Hall Effect sensors as detectors. The magnetoresistive gear tooth sensor possesses the characteristics of wide frequency bandwidth, high resolution by using small gear modulus, small sensing distance and higher price [6-7]. Hall Effect gear tooth sensor has the advantages of large measuring range, wide frequency bandwidth, simple structure, larger sensing distance and low price [2-5]. Therefore they find more applications than magnetoresistive sensors.

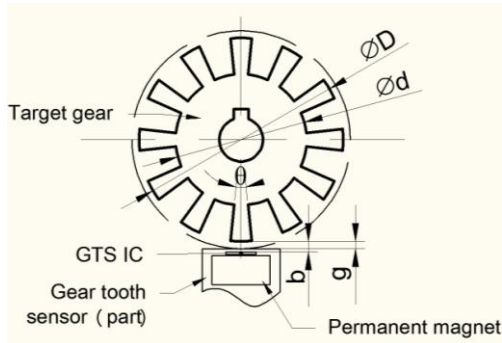
The sensing distance of Hall Effect gear tooth sensors, however, is too small in case of using small gear modulus. This is a problem especially when the measured rotational machines have strong vibration. Therefore the parameters, such as sensing distance, duty cycle and

phase drift of Hall Effect gear tooth sensors should be optimized by using magnetic field analysis, experiments and mathematical models [1].

2. Hall Effect Gear Tooth sensors

2.1. Gear Tooth Sensors with Single Output

A rotational speed measuring system consists of a Hall Effect gear tooth sensor (GTS) IC, a permanent magnet and a target gear wheel. The GTS IC detects the addendum or slot of the target wheel by using peak magnetic field (Fig. 1) or differential magnetic field (Fig. 2) principles [2-3]. It generates one channel of output impulses when the target wheel rotates.



- D : diameter of the addendum cycle
- d : diameter of the dedendum cycle
- g : sensing gap between the gear addendum and sensor's end
- b : sensing distance between the gear addendum and sensing center of GTS IC

Fig. 1 Rotational speed measuring system based on peak magnetic field detection

In the peak magnetic field detection the GTS IC has only one Hall Effect element [3]. It detects the peak value of magnetic flux density, which changes in sinusoidal form during the target gear rotates, and generates a square wave. However, GTS IC based on the peak value detection has a small sensing distance.

The sensing distance can be increased by using GTS IC based on differential magnetic field detection. In this case sensing gap/distance is nearly doubled in comparison with the former one. It is more convenient for installation of the gear tooth sensors.

The differential gear tooth sensor model is shown in Fig.2. Two Hall Effect elements, which are positioned in distance a , are used for detecting the magnetic field change during the rotation of the target wheel. The GTS IC generates output impulses by using the difference between the two output voltages of the two Hall Effect elements caused by differential magnetic field [2].

According to differential magnetic field detection [2], the geometric duty cycle of the target wheel can be determined by:

$$\eta_g = \frac{N\theta}{360} \quad (1)$$

The duty cycle of the output signal of the Gear Tooth Sensor can be estimated by [1]

$$\eta = \frac{\delta L_1}{L} = \frac{\delta L_1 N}{\pi(D + 2b)} \quad (2)$$

where δ is edge effect coefficient, L_1 is addendum arc width, L is effective tooth arc pitch, D

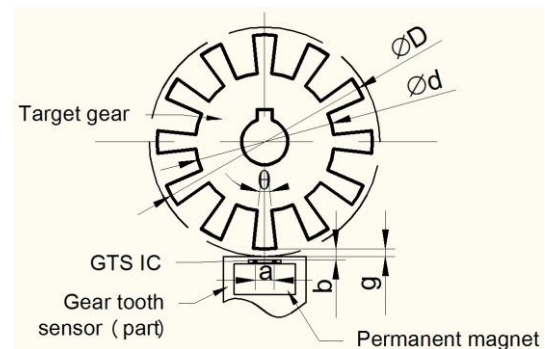
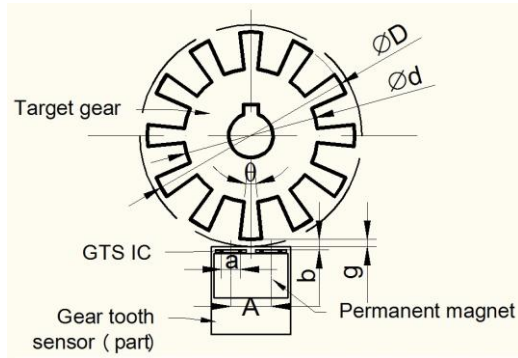


Fig. 2 Rotational speed measuring system based on differential magnetic field detection

is diameter of addendum cycle of the target wheel, b is sensing distance between the gear addendum and sensing center of GTS IC and N is the number of teeth. The edge effect coefficient δ can be determined by experiment [1].

2.2. Gear Tooth Sensors with Double Outputs

The rotational direction cannot be determined by sensor shown in Fig. 1. In order to detect the rotational direction an additional Hall Effect GTS IC must be used in the measuring system. Fig.3. shows a Hall Effect rotational speed and direction measuring system. This system has two channels of output impulses.



- D : diameter of the addendum cycle
- d : diameter of the dedendum cycle
- g : sensing gap between the gear addendum and sensor's end
- b : sensing distance between the gear addendum and sensing center of GTS IC
- a : distance between the Hall Effect elements in each GTS IC
- A : distance between the centerlines of the two GTS ICs

Fig. 3 Rotational speed and direction measuring system based on differential GTS ICs

The duty cycle η of each output signal can be calculated by (2). The phase drift, $\Delta\Phi$, between the two electrical output signals can be determined by [1]:

$$\begin{aligned} \Delta\phi &= \phi_2(\text{Output}_2) - \phi_1(\text{Output}_1) \\ &= \frac{360^\circ N}{\pi} \sin^{-1}\left(\frac{\underline{A}}{\sqrt{(D+2b)^2 + \underline{A}^2}}\right) \end{aligned} \quad (3)$$

where the distance vector A is defined by

$$\underline{A} = \begin{cases} A & \text{counter clockwise rotation} \\ -A & \text{clockwise rotation} \end{cases} \quad (4)$$

Equation (3) can be simplified as follows

$$\Delta\phi = \frac{360^\circ N}{\pi} \tan^{-1}\left(\frac{\underline{A}}{D+2b}\right) \quad (5)$$

3. Parameter Optimization

3.1. Sensing Distance

The sensing distance b or gap g can be optimized by selecting suitable Hall Effect GTS IC and by optimizing the geometry and material of the permanent magnet and sensor case. GTS IC detects the target wheel by using differential magnetic field [2] and peak magnetic field [3]. The GTS IC using differential magnetic field has a better sensing distance. A new sensor CYGTS101DC-S is developed with GTS IC using differential magnetic field detection and optimized with improved permanent magnet in order to increase the sensing distance.

Three GTS sensors 1GT101DC, CYGTS101DC and CYGTS101DC-S are used for comparison experiments. Under using target gear 1 ($D=28\text{mm}$, $d=22\text{mm}$, $N=22$, $\theta=8.18^\circ$), the duty cycle of the output signal of the sensors are measured in different sensing gap g . 15 repeat measurements are made for each sensing gap. The mean value x_η and standard deviation σ_η of the duty cycle are calculated with the repeat measured values. The calculated mean duty cycle of each sensor are given in Table 1 to Table 3.

Table 1 Results of sensor Honeywell 1GT101DC using peak magnetic field detection

Sensing gap g (mm)	0.5	0.6	0.7
Duty cycle x_η (%)	43.6	51.4	58.6
Standard deviation σ_η	5.56	7.48	5.66

Table 2 Results of sensor CYGTS101DC using peak magnetic field detection

Sensing gap g (mm)	0.5	0.6	0.7	1.0
Duty cycle x_η (%)	48.4	45.5	47.4	50.5
Standard deviation σ_η	1.37	2.16	2.40	4.76

Table 3 Results of sensor CYGTS101DC-S using differential magnetic field detection

Sensing gap g (mm)	0.5	1.0	1.5	2.0	2.5
Duty cycle x_η (%)	50.2	50.6	50.6	51.0	56.1
Standard deviation σ_η	2.47	3.30	2.17	2.09	2.52

Fig. 4 and Fig. 5 show the mean duty cycle and the standard deviation of the three sensors, respectively. From the results mentioned above it can be concluded that the optimized sensor CYGTS101DC-S has better sensing distance. Its maximum sensing distance is 2.5mm under using the target gear 1.

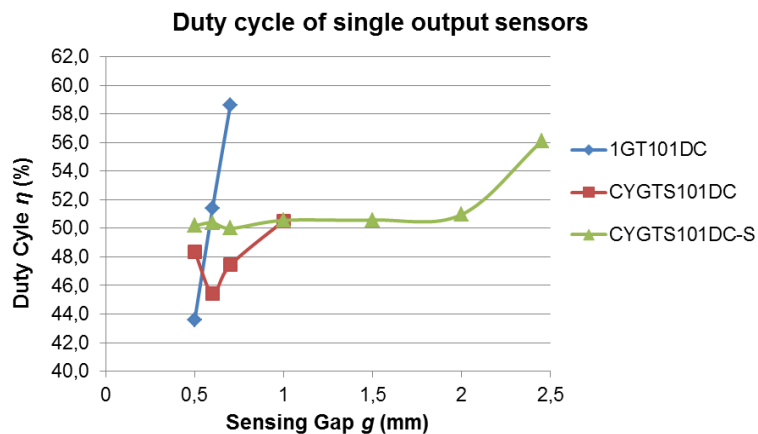


Fig. 4 The average value of duty cycle of the three GTS sensors under test

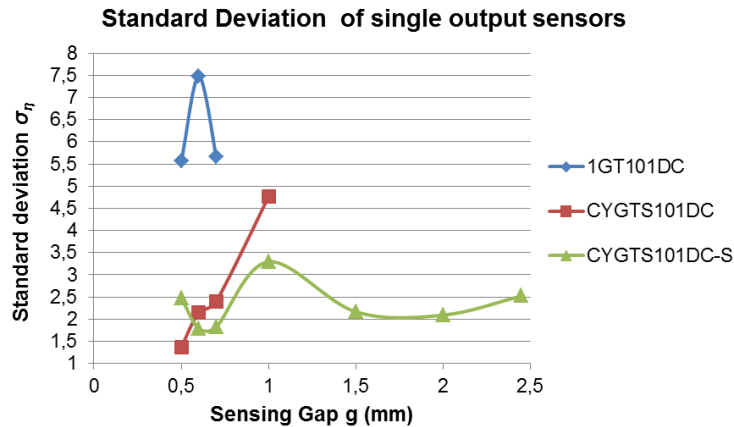


Fig. 5 The standard deviation of duty cycle of the three GTS sensors under test

3.2. Duty Cycle

For dual outputs sensors, the duty cycle η depends on the geometry of target gear wheel and the sensing distance. It can be optimized by using model (2). The best duty cycle is 50% for the most applications. Therefore model-based design is introduced to the optimization of the target wheel in order to get the best duty cycle.

Basically, according to geometrical duty cycle (1), the addendum and dedendum arc angles should be the same. In addition, the middle radius arc should be suitable to the distance a , which is related to the number of teeth. From many experimental results, target gear should have more than 10 teeth. Thus target gears with 12 and 22 teeth are mainly used in experiments described in this paper

The shape of tooth also influences the duty cycle. Fig. 6 is target wheel with common tooth shape. Fig. 7 shows a target gear with another new tooth shape. Table 4 and 5 and Fig. 8 and 9 show the results tested by the two target gears.

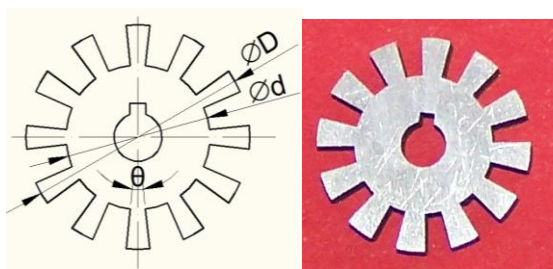


Fig. 6 Target gear with common tooth shape

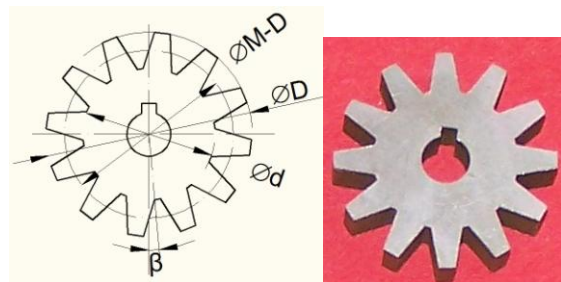


Fig. 7 Target gear with new tooth shape

Table 4 Sensor CYGTS104U-S tested with common tooth shape ($D=28$, $d=18$, $N=12$, $\theta=12^\circ$)

Sensing gap g (mm)	0.5	1.0	1.5	2.0	2.5	3.0	3.5
Duty cycle $x_{\eta 1}$ (%)	48.5	48.7	50.0	49.8	51.9	52.1	54.2
Duty cycle $x_{\eta 2}$ (%)	50.6	51.0	51.2	52.0	51.6	53.2	55.5
Difference $x_{\eta 2} - x_{\eta 1}$ (%)	2.1	2.3	1.2	2.2	-0.3	1.1	1.3

Table 5 Sensor CYGTS104U-S tested with new tooth shape ($D=28$, $d=18$, $N=12$, $\beta=5^\circ$)

Sensing gap g (mm)	0.5	1.0	1.5	2.0	2.5	3.0	3.5
Duty cycle x_{η_1} (%)	51.2	50.5	50.2	50.1	51.4	52.8	55.3
Duty cycle x_{η_2} (%)	50.1	49.2	50.3	50.7	50.8	51.6	55.6
Difference $x_{\eta_2}-x_{\eta_1}$ (%)	-1.1	-1.3	0.1	0.6	-0.6	-1.2	0.3

The difference between the two duty cycles of the sensor CYGTS104U-S under using target gear with the new tooth shape is smaller than that of using target gear with common tooth shape.

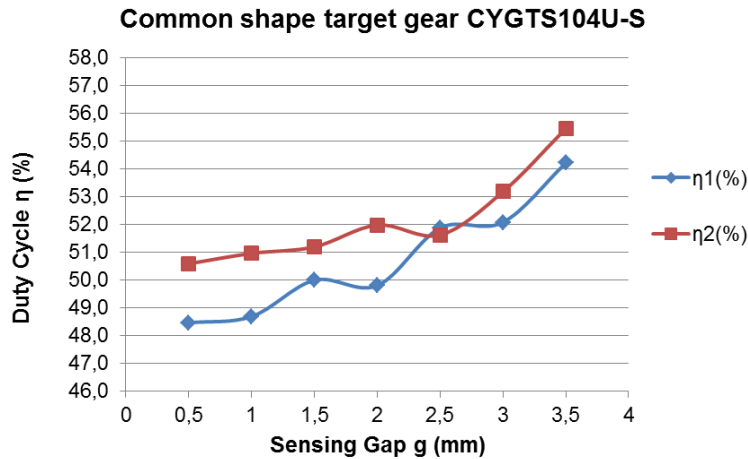


Fig. 8 Test results using target gear with common tooth shape shown in Fig. 6

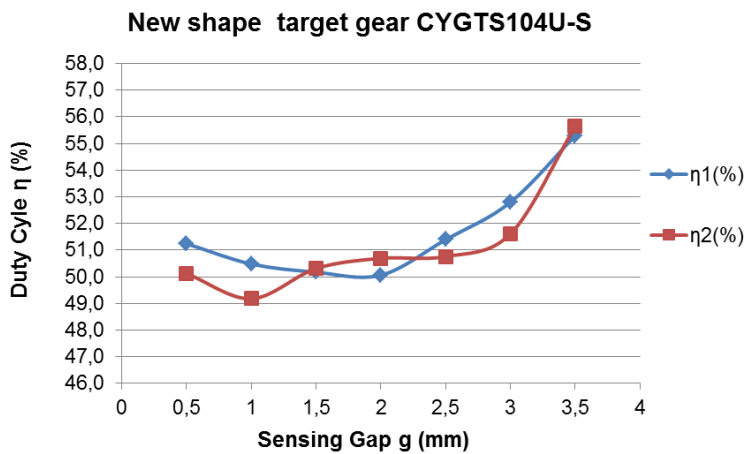


Fig. 9 Test results using target gear with new tooth shape shown in Fig. 7

3.3. Phase Drift

The Phase Drift Φ of the two output signals are dependent on the distance between the two GTS ICs and on the geometry of target gear. It can be optimized by the model (3)-(5). The best phase drift is 90° for easy determination of rotational direction. Model-based design is

also important for obtaining the best phase drift. Tables 6-9 show a comparison of optimized sensor CYGTS104X to no-optimized sensors.

Table 6 indicates the measured parameters of Honeywell sensor SNDH-T4L-G01 without parameter optimization. The target wheel ($N=64$, $D=81.5\text{mm}$, $L_1=L_2$) is designed for this sensor in order to get duty cycle of 50% and phase drift of 90° according to (2) and (3) without considering the sensing distance b . The maximum deviation of phase drift and duty cycle is 7.78% and 6.0%, respectively. The maximal sensing gap of this sensor is only about 0.8mm.

Table 7 presents the measured parameters of sensor CYGTS104X after optimization. The distance between the two Hall Effect GTS ICs of the sensor CYGTS104X is 1.2mm. By using the same target wheel the phase drift is 107.98° according to (3) without considering the sensing distance b and the duty cycle is about 50%. The maximum deviation of phase drift and duty cycle is -1.83% and 4.0%, respectively. The maximum sensing gap of this sensor is about 2.0mm.

Table 8 shows the results of sensor CYGTS104U-S with distance between the two Hall ICs of 5.4mm. The deviations of phase drifts and duty cycles of the three sensors are given in the Table 9. It is obviously that the deviation of phase drift of the sensor CYGTS104U-S is much higher than that of other two sensors. The reason is that the distance $a=5.4\text{mm}$ is not suitable for mathematical model (5) under using the target wheel.

Therefore the performances of sensor CYGTS104X after optimization are better than those of sensor SNDH-T4L-G01 and CYGTS104U-S without optimization.

Table 6 Measured Parameters of Honeywell SNDH-T4L-G01 ($N=64$, $D=81.5\text{mm}$, $L_1=L_2$, $a=1\text{mm}$)

Speed	Phase drift ($^\circ$)	Duty cycle (%)	Max. sensing gap g (mm)
1500rpm	83	50.0	0.8
3000rpm	94	53.0	0.8

Table 7 Measured parameters of sensor CYGTS104X ($N=64$, $D=81.5\text{mm}$, $L_1=L_2$, $a=1.2\text{mm}$)

Speed	Phase drift ($^\circ$)	Duty cycle (%)	Max. sensing gap g (mm)
1500rpm	107	52.0	2.0
3000rpm	106	50.0	2.0

Table 8 Measured parameters of sensor CYGTS104U-S ($N=64$, $D=81.5\text{mm}$, $L_1=L_2$, $a=5.4\text{mm}$)

Speed	Phase drift ($^\circ$)	Duty cycle (%)	Max. sensing gap g (mm)
1500rpm	45	51.3	1.6
3000rpm	46	50.0	1.6

Table 9 Deviations of phase drifts and duty cycles of the three sensors

Speed	SNDH-T4L-G01 (%)		CYGTS104X (%)		CYGTS104U-S (%)	
	Phase drift	Duty cycle	Phase drift	Duty cycle	Phase drift	Duty cycle
1500rpm	-7.78	0.00	-0.91	4.00	-17.85	2.60
3000rpm	4.44	6.00	-1.83	0.00	-16.03	0.00

Using the optimized sensor CYGTS104X and the 12 teeth target gear with the new tooth shape shown in Fig. 7 one can get relative stable duty cycle and phase drift in the sensing gap of 0.5-4mm. Table 10 indicates the measured results.

Table 10 Measured results of sensor CYGTS104X with target gear shown in Fig. 7

Sensing gap g (mm)	0.5	1.0	1.5	2.0	2.5	3.0	3.5	4.0
Duty cycle $x_{\eta 1}$ (%)	50.3	51.2	50.8	51.3	50.7	51.9	52.9	57.9
Duty cycle $x_{\eta 2}$ (%)	50.3	49.3	50.2	48.8	51.9	52.0	55.3	58.8
Phase drift $\Delta\Phi$ (°)	91.7	101.0	104.3	112.4	109.7	111.0	107.8	107.2

4. Conclusions

In this paper the optimization of Hall Effect gear tooth speed sensors are discussed. From the experiments results of sensor optimization one can draw the following conclusions:

- The sensing gap/distance of Hall Effect Gear Tooth sensors can be improved by using differential magnetic field detection. In this case the sensing gap of single output sensors is 2.5 times of that by using peak magnetic field detection.
- For dual output sensors the sensing gap/distance depends not only on the magnetic field detection method but also on the distance between the two Hall ICs (see table 9 and 10). The sensors with smaller distance a have better sensing gap.
- The duty cycle of Hall Effect gear tooth sensors depends on the geometric duty cycle (1) and tooth shape of the target wheel and the magnetic field detection method. Sensors with differential magnetic field detection and using target wheel shown in Fig. 7 have stable duty cycle.
- The phase drift of dual output sensors can be determined by the mathematical model (3)-(5) more accurately if the sensors are made according to differential magnetic field detection and by using a smaller distance between the two Hall GTS ICs.

5. Literatures

- [1] J-G., Liu and Z. Zheng, Mathematical Models of Gear Tooth Speed Sensors with Dual Outputs, Joint International IMEKO TC1+TC7+TC13 Symposium, August 31st-September 2nd, 2011, Jena, Germany, urn:nbn:de:gbv: ilm1-2011imeko:2, proceedings, pp. 82-86
- [2] Infineon Technologies, TLE4921-5U Dynamic Differential Hall Effect Sensor IC, data sheet, <http://www.infineon.com>
- [3] Melexis, MLX90254 Differential Dynamic Hall Effect Sensor, data sheet, <http://www.melexis.com>
- [4] Honeywell, GT1 Series Hall Effect Gear Tooth Sensors, <http://honeywell.com/Pages/Home.aspx>
- [5] Honeywell, SNDH Series Quadrature General Industrial Speed and Direction Sensors, 000641-2-EN IL50 GLO, USA, October 2007, <http://www.honeywell.com/sensing>
- [6] Siemens AG, Differential Magnetoresistive Sensor, FP 210 D 250-22, www.datasheetcatalog.com
- [7] Fritz Schmeißer, Klaus Dietmayer, APPLICATION NOTE of Rotational Speed Sensors KMI15/16, Philips Semiconductors, Philips Electronics N.V. 1999
- [8] ChenYang Technologies GmbH and Co. KG., "Hall Effect Gear Tooth Sensor CYGTS101DC", data sheet, <http://www.hallsensors.de/CYGTS101DC.pdf>
- [9] J.-G. Liu, "Hall Effect Gear Tooth Sensors CYGTS104", data sheet, ChenYang Technologies GmbH and Co. KG., <http://www.hallsensors.de/CYGTS104.pdf>

Authors:

B.Sc. Junwen LU, postgraduate Student, University of Shanghai for Science and Technology (USST), Jungong Load 516, 200093 Shanghai, P.R. China, louis.lu@chenyang.de. Ms Lu does her Master Thesis at ChenYang Technologies GmbH & Co. KG since November 1, 2011

Dr.-Ing. habil. Ji-Gou Liu, general and technical manager, ChenYang Technologies GmbH & Co. KG., Markt Schwabener Str. 8, 85464 Finsing, Germany, Tel.: +49-8121-2574100, Fax: +49-8121-2574101, jigou.liu@chenyang-ism.com, <http://www.chenyang-ism.com>.